PL-TR-94-2206

RESEARCH INTO ARTIFICIALLY INDUCED ATMOSPHERIC DISTURBANCES

J. W. Duff and F. Bien

Spectral Sciences, Inc.
99 South Bedford Street, #7
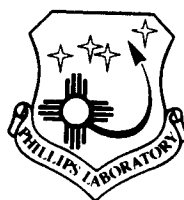Burlington, MA 01803-5169

DTIC
ELECTE
JAN 31 1995
S
G
D

June 1994

19950127 160
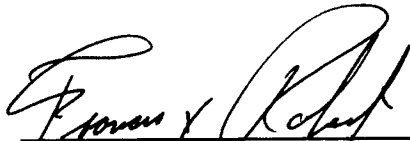
Scientific No. 1

PHILLIPS LABORATORY
Directorate of Geophysics
AIR FORCE MATERIEL COMMAND
HANSCOM AFB, MA 01731-3010

"This technical report has been reviewed and is approved for publication"

FRANCIS X. ROBERT
Contract Manager

STEPHAN D. PRICE
Branch Chief

ROGER A. VAN TASSEL
Division Director

This report has been reviewed by the ESC Public Affairs Office (PA) and is releasable to the National Technical Information Service (NTIS).

Qualified requestors may obtain additional copies from the Defense Technical Information Center (DTIC). All others should apply to the National Technical Information Service (NTIS).

If your address has changed, if you wish to be removed from the mailing list, or if the addressee is no longer employed by your organization, please notify PL/TSI, 29 Randolph Road, Hanscom AFB, MA 01731-3010. This will assist us in maintaining a current mailing list.

Do not return copies of this report unless contractual obligations or notices on a specific document requires that it be returned.

REPORT DOCUMENTATION PAGE

Public reporting burden for this collection of information is estimated to average 1 hour per response, including the time for reviewing instructions, searching existing data sources, gathering and maintaining the data needed, and completing and reviewing the collection of information. Send comments regarding this burden estimate or any other aspect of this collection of information, including suggestions for reducing this burden, to Washington Headquarters Services, Directorate for Information Operations and Reports, 1215 Jefferson Davis Highway, Suite 1204, Arlington, VA 22202-4302, and to the Office of Management and Budget, Paperwork Reduction Project (0704-0188), Washington, DC 20503.

1. AGENCY USE ONLY (Leave blank)	2. REPORT DATE	3. REPORT TYPE AND DATES COVERED
	June 1994	Scientific #1

4. TITLE AND SUBTITLE

Research into Artificially Induced Atmospheric Disturbances

5. FUNDING NUMBERS

C — F19628-93-C-0052
PE — 62101
PR — 5322
TA — GG
WU — BE

6. AUTHOR(S)

James W. Duff and Fritz Bien

7. PERFORMING ORGANIZATION NAME(S) AND ADDRESS(ES)

Spectral Sciences, Inc.
99 South Bedford Street, #7
Burlington, MA 01803-5169

8. PERFORMING ORGANIZATION REPORT NUMBER

SSI-TR-246

9. SPONSORING/MONITORING AGENCY NAME(S) AND ADDRESS(ES)

Phillips Laboratory
29 Randolph Road
Hanscom AFB, MA 01731-3010

Contract Monitor: Frank X. Robert/GPOB

10. SPONSORING/MONITORING AGENCY REPORT NUMBER

PL-TR-94-2206

11. SUPPLEMENTARY NOTES

12a. DISTRIBUTION/AVAILABILITY STATEMENT

Approved for public release; distribution unlimited

12b. DISTRIBUTION CODE

13. ABSTRACT (Maximum 200 words)

A detailed chemical kinetics model describing the interaction of an electron beam with the atmosphere is used to study the effects of the reaction of translationally hot $N(^4S)$ atoms with O_2 on NO formation and emission during the EXCEDE III artificially auroral experiment. The rate constants and vibrational distributions for rotationally hot NO are obtained from extensive quasiclassical trajectory calculations for the $N(^4S) + O_2$ reaction using realistic ab initio potential energy surfaces. It is shown that a quantitative description of rotationally thermal and hot NO emission observed in EXCEDE III requires the inclusion of hyperthermal N atom chemistry in our chemical kinetics model. This analysis provides the first quantitative evidence of the importance of hyperthermal $N(^4S)$ and $N(^2D)$ atoms in the formation of vibrationally and rotationally excited NO. Excellent agreement between the chemical kinetics model developed for EXCEDE and the vibrational populations derived from the interferometer data is obtained under conditions of thermalization of nitrogen atoms (i.e., at 103 km under max dose conditions). Analysis of the vibrational populations from the interferometer under other conditions indicate that hyperthermal $N(^2D)$ atoms also play an important role in NO formation.

14. SUBJECT TERMS

Artificial Aurora   hyperthermal
vibrational/rotational excitation quasiclassical trajectory

15. NUMBER OF PAGES

26

16. PRICE CODE

17. SECURITY CLASSIFICATION OF REPORT	18. SECURITY CLASSIFICATION OF THIS PAGE	19. SECURITY CLASSIFICATION OF ABSTRACT	20. LIMITATION OF ABSTRACT
UNCLASSIFIED	UNCLASSIFIED	UNCLASSIFIED	SAR

NSN 7540-01-280-5500

Standard Form 298 (Rev 2-89)
Prescribed by ANSI Std. Z39-18
298-102

TABLE OF CONTENTS

LIST OF ILLUSTRATIONS

Accesion For		
NTIS CRA&I	☒	
DTIC TAB	☐	
Unannounced	☐	
Justification		
By		
Distribution /		
Availability Codes		
Dist	Avail and / or Special	
A-1		

1. INTRODUCTION

This first annual report describes work done during the period May 6, 1993 through May 5, 1994. The objective of this program is to develop a phenomenological chemical-kinetics database for the nuclear-disturbed atmosphere. To this end, the comparison of data from the EXCEDE III experiment to a robust chemical kinetics model which contains the current state of knowledge of electron-atmospheric interactions will ultimately provide the information necessary for predicting nuclear effects on systems. Current uncertainties in the phenomenological models based on reaction rate coefficients and calculated electron concentrations that affect infrared emissions are thought to lie within a factor of 2 or 3 in the best known situations and much worse in many other cases. Unknowns, or disputed reaction rates, include fractional yields of species such as $N(^2P)$ and $N_2(A)$, effects of these species in the disturbed atmosphere, and creation mechanisms for species such as rotationally excited NO. Emissions due to very high rotation levels which are not quenched in the atmosphere may have a great impact on the atmospheric bandpasses where current surveillance instruments are being designed.

The major effort during this period has been the analysis of electron-beam enhanced $NO(\Delta v = 1)$ emission observed by the three circular-variable filter (CVF) spectrometers and interferometer during EXCEDE III. In addition to considering the traditional $N(^2D) + O_2$ reaction at thermal energies, the chemistry of translationally hot N atoms in NO formation has been investigated in detail, with emphasis on the hyperthermal $N(^4S) + O_2$ reaction. It has been shown that a quantitative description of rotationally thermal and hot NO emission observed in EXCEDE III requires the inclusion of hyperthermal N atom chemistry in our chemical kinetics model.

Section 2 discusses the evidence for the importance of the reactions of hyperthermal $N(^4S)$ and $N(^2D)$ with O_2 in producing NO. The chemical dynamics of the $N(^4S) + O_2$ reaction is discussed in Section 3, and preliminary calculations of NO vibrational populations using a hyperthermal nitrogen atom kinetics model is presented in Section 4. A brief summary is given in Section 5.

1

2. IMPORTANCE OF TRANSLATIONALLY HOT NITROGEN ATOMS

The reactions of metastable nitrogen atoms with molecular oxygen are thought to be the major source of nitric oxide chemiluminescence in the thermosphere.[1] Earlier models of NO formation assumed that the chemistry of $N(^2D)$ is the most significant contributor to NO formation, while the relaxation of $N(^2P)$ to $N(^2D)$ and the reaction of $N(^2P)$ with O_2[2] make a relatively minor contribution in the thermospheric dayglow[3] and aurora.[4-5]

Analysis of the EXCEDE III CVF NO data at apogee (115 km) has provided strong evidence for a mechanism(s) of NO formation in addition to the thermal reaction

$$N(^2D) + O_2 \rightarrow NO(v) + O \ . \tag{1}$$

Reaction (1) has previously been considered as a source of rotationally thermal NO. The source of rotationally hot NO is currently unknown, although it has been suggested that the reaction of $N(^2P)$ with O_2 is a possible source. We have shown previously that this process

$$N(^2P) + O_2 \rightarrow NO(v,T_r) + O \tag{2}$$

can not be a source of rotationally thermal or hot NO emission in EXCEDE III. To quantify this discussion, a comparison of the CVF data at 115 km (apogee) with the EXCEDE kinetic model using Reaction (1) as the only source of $NO(\Delta v = 1)$ emission is shown in Figure 1. Although the disagreement between the model and data at 0.2 s (8° CVF) and 0.5 s (20° CVF) could be due to uncertainties in the atmospheric profiles, it is clear that the disagreement at 0 s (0° CVF) results from the inability of Reaction (1) to explain NO emission. Further evidence of the inadequacy of Reaction (1) is provided by the analysis of the interferometer data at apogee which shows significant emission from highly rotationally excited NO. Furthermore, at apogee, Reaction (1) does not produce the correct NO vibrational distribution to explain the rotationally thermal populations obtained from the interferometer data.
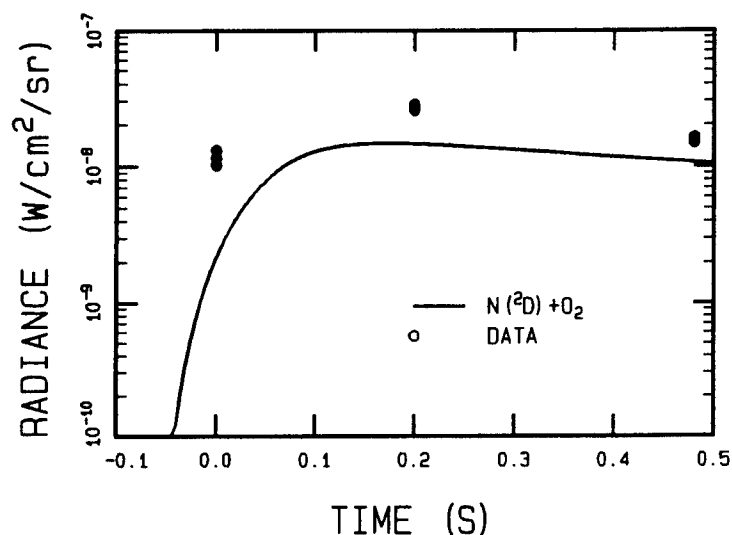
Figure 1. Comparison of the CVF Data in the NO($\Delta v = 1$) Bandpass with the EXCEDE Kinetic Model at 115 km Using the Thermal N(^{2}D)+O$_2$ Mechanism.

Thus, it would appear that another mechanism for the creation of NO(v) is necessary to explain the data near apogee. Recently, it has been suggested that the reaction of translationally hot N(^{4}S) with O$_2$ is an important contributor to NO formed in the thermosphere.[6-7] Furthermore, Sharma et al.[8] have performed a calculation that shows the importance of the N(^{4}S)+O$_2$ reaction in recent observations of highly rotationally excited NO vibrational emissions in the dayglow.[9,10] Their calculation was based on two recent studies; a quasiclassical trajectory study of N(^{4}S) + O$_2$ by Gilibert et al.[11] indicating that the N(^{4}S) reaction produces NO in high ro-vibrational states at a nearly gas kinetic rate, and the calculated nonthermal thermospheric N(^{4}S) translational energy distribution of Shematovich et al.[12]

3. CLASSICAL DYNAMICS OF THE $N(^4S)+O_2(X^3\Sigma_g^-) \rightarrow NO(X^2\Pi)+O(^3P)$ REACTION

3.1 Introduction

The only published experimental data on the $N(^4S)+O_2$ reaction are thermal rate constant measurements,[13] which are only reliable up to 1500 K, and the NO vibrational distribution at room temperature.[14-16] The dependence of the reaction rate and final state distributions on the initial translational, vibrational, or rotational energy has only been calculated on the ground state potential energy surface. Furthermore, the internal energy distribution of the $NO(X^2\Pi)$ product is not completely characterized for hyperthermal collisional energies. The present theoretical study determines the reaction rate constant and the nascent NO vibrational-rotational distributions formed by the translationally hot $N(4S)+O_2$ reaction as a function of $N(^4S)$ translational energy from 0.5 to 2.75 eV. The results of this study provide the reaction attributes of $N(^4S)+O_2$ useful for modeling the production of NO from "hot" $N(^4S)$[7,17-18] and the NO dayglow emission spectra.[8-10]

3.2 Previous Theoretical Work

The reaction of $N(^4S)+O_2(X\ ^3\Sigma_g^-)$ to form $NO(X^2\Pi)+O(^3P)$ is exothermic by 1.38 eV and occurs on two electronic potential energy surfaces of $^2A'$ and $^4A'$ symmetry (neglecting spin-orbit coupling). The electronic degeneracies are such that 4/12 of the $N(^4S)+O_2$ collisions occur on the $^4A'$ surface compared to 2/12 on the ground state $^2A'$ surface. The remaining 6/12 of the collisions occur on the $^6A'$ surface which does not correlate with the ground state products $NO(X^2\Pi)+O(^3P)$, and is not further considered. An extensive set of *ab initio* quantum mechanical calculations for the $^2A'$ and $^4A'$ potential energy surfaces have been carried out by Walch and Jaffe[19] to characterize the saddle point geometries and to a lesser extent the minimum energy path. The lowest $^2A'$ potential energy surface, which has an estimated activation energy of approximately 0.3 eV,[13] makes the dominant contribution to the reaction rate for temperatures below 1500 K. Although the $^4A'$ surface, which has an estimated barrier

of 0.65 eV,[19] does not contribute to the reaction rate for temperatures below 1500 K, it must be considered for the translationally "hot" $N(^4S)$ reaction channel.

There have been two previous quasiclassical trajectory calculations reported for the $N(^4S)+O_2$ reaction. The first study was performed by Jaffe et al.[20] using the $^2A'$ and $^4A'$ surfaces mentioned above. However, their study emphasizes the thermal reaction rate constant at high temperatures and, although consistent with experiment, do not provide rate constants as a function of collision energy or final state distributions of the products. The second quasiclassical trajectory study by Gilibert et al.[11] only considered the lowest $^2A'$ potential energy surface, and therefore is applicable to thermal collisions below 1500 K or collision energies less than approximately 0.75 eV. More importantly, the fitting of an analytical functional form to the calculated *ab initio* $^2A'$ potential energy surface introduced an artificial barrier of approximately 0.55 eV in the reactant channel, which implies that the calculated threshold for reaction is too high by approximately 0.22 eV. Thermal rate constants calculated using the $^2A'$ PES of Gilibert et al. would result in an activation energy approximately 5 kcal/mole higher than experiment. Therefore, we have carried out extensive quasiclassical trajectory calculations[21] using a new analytical fit to the $^2A'$ and $^4A'$ *ab initio* potential energy surfaces of Walch and Jaffe[19] to predict the reaction attributes of $N(^4S)+O_2$.

3.3 Methodology

The most recent *ab initio* calculations of Walch and Jaffe[19] for the $^2A'$ and $^4A'$ potential energy surfaces (PES) are used as a basis for the analytical representation of the $N(^4S)+O_2$ reaction. The study of Walch and Jaffe involved a total of 66 *ab initio* points for the $^2A'$ surface and 23 for the $^4A'$ surface at the complete active space self-consistent field (CASSCF) level followed by multireference contracted configuration interaction (CCI) calculations. The "best" theoretical estimate of the barrier height for the $^2A'$ surface was estimated to be 2-3 kcal/mole too high compared to the experimental activation energy. In our model, the calculated *ab initio* points in the vicinity of the saddle point were adjusted by a constant factor such that the barrier heights for the $^2A'$ and $^4A'$ are in agreement with the experimental estimate for the $^2A'$ surface[13] and theoretical estimate for the $^4A'$ surface.[19] The adjusted *ab initio* points were then fit to an

5

analytical representation of the potential energy surface suggested by Sorbie and Murrell[22] using a nonlinear least squares method. Care was taken to ensure that the fitting process did not introduce any spurious artifacts in the resulting analytical functions. The resultant barrier heights of the analytical functions are 0.3 eV and 0.65 eV for the $^2A'$ and $^4A'$ potential energy surfaces, respectively. The location and the angular dependence of the barriers are also accurately reproduced, with a standard deviation of the nonlinear fits for both surfaces of 0.047 eV.

The quasiclassical trajectory (QCT) method is used to compute the reaction rate constants and the final vibrational and rotational state distributions.[21] The validity of classical mechanics for calculating reaction rate constants and product distributions has been discussed elsewhere.[21] Classical calculations are expected to be reliable at energies greater than the barrier heights, where quantum effects such as tunneling may be important, for state-to-state rate constants which are strongly classically allowed. Calculations are carried out separately for the $^2A'$ and $^4A'$ potential energy surfaces and then averaged together with the degeneracy factors of ½ and ⅓, respectively. Standard Monte Carlo techniques are used to compute the thermal reaction rate constant as a function of temperature, where the translational energy and the initial (v, j) states are chosen from Boltzmann distributions. Reaction rate constants and final (v', j') distributions are also calculated as a function of initial translational energy in the range of 0.5-2.75 eV with the initial (v, j) states selected from a 300 K Boltzmann distribution. The classical equations of motion are integrated using a variable step size predictor-corrector method.[23] The final vibrational and rotational quantum numbers (v', j') are obtained from the correspondence rules $v'_{cl} = (v' + ½)h$ and $j'_{cl} = (j' + ½)\hbar$, where v'_{cl} and j'_{cl} are the classical vibrational and rotational action variables. The final (v', j') distributions are then obtained using the standard histogram method. A total of 580,000 (330,000 for the $^2A'$ PES and 250,000 for the $^4A'$ PES) trajectories are used in the current study.

3.4 Results and Discussion

Quasiclassical trajectory thermal reaction rate constants are computed for the temperature range of 500 K to 5000 K. A comparison of the calculated thermal rate constant, k(T), with a
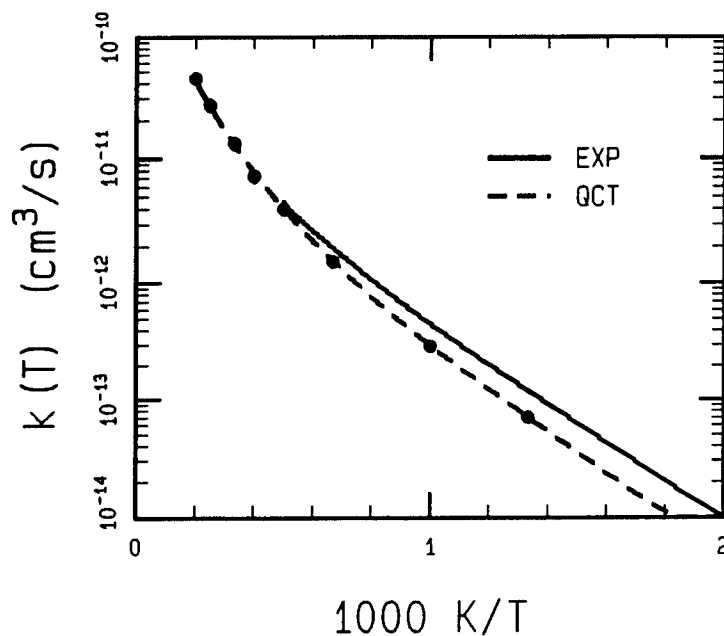
6

Figure 2. Comparison of the Experimental (EXP) and Quasiclassical Trajectory (QCT) Thermal Rate Constants as a Function of Temperature.

recommended fit to the available kinetic data[13] is shown in Figure 2. The QCT thermal rate constant agrees well with the experimental measurements over the entire temperature range, although the calculations consistently underpredict the rate constants below 1250 K. This systematic disagreement is probably due to two factors: either the barrier height of 0.3 eV is still too high, or, owing to the rather large barrier, there is a significant contribution from quantum mechanical tunneling, which cannot be accounted for with the QCT method. Although of critical importance for determining low temperature thermal rate constants, neither one of these concerns should be as significant for calculation of the high energy (>0.5 eV) rate constants and final state distributions reported here. The comparison in Figure 2 also points out the difficulty in extrapolating low temperature rate constants to higher temperature, where a significant contribution to the rate constant may come from a mechanism or potential energy surface not important at lower temperatures. In particular, the present calculations indicate that if the lower temperature rate constant (only $^2A'$) is extrapolated to estimate the reaction rate constant at 5000 K, the total rate constant would be underestimated by a factor of 2. It should also be mentioned
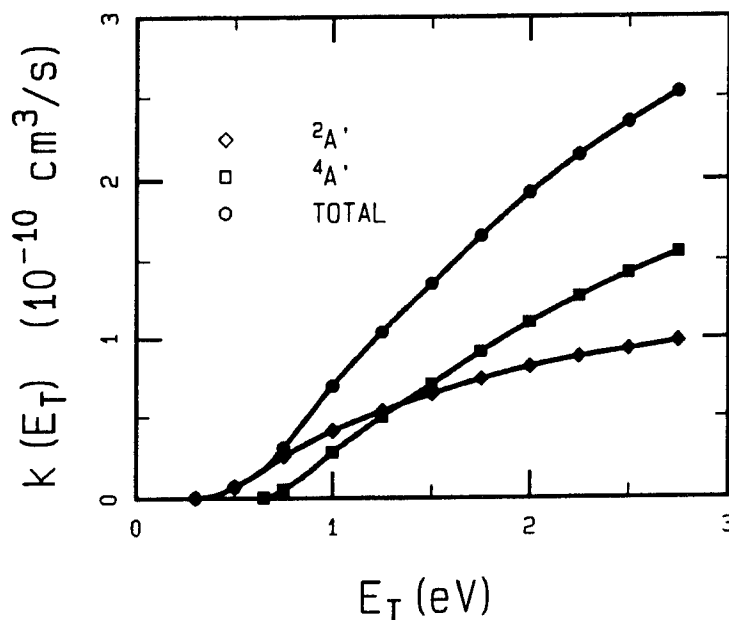
7

$k(E_T)$ $(10^{-10}$ cm^3/S)

◇ $^2A'$
□ $^4A'$
○   TOTAL

E_T (eV)

Figure 3.   Contribution of the QCT Rate Constants for the $^2A'$ and $^4A'$ Potential Energy Surfaces to the Total Rate Constant as a Function of the Initial Relative Translational Energy.

that the present results are in good agreement with the rate constants calculated by Jaffe et al.[20] using a completely different analytical form for the potential energy surfaces.

A more useful quantity for the thermospheric NO production models[7,17-18] is the reaction rate constant, $k(E_T)$, as a function of initial translational energy, E_T. Figure 3 shows the total reaction rate constant calculated as a function of E_T. The initial O_2 vibrational and rotational states were averaged over a Boltzmann distribution at 300 K. Also shown in Figure 3 is the individual contribution of the $^2A'$ and $^4A'$ potential energy surfaces to the rate constant. As expected, the reaction rate is dominated by the $^2A'$ PES for energies below 1 eV. As the initial translational energy is increased, the relative importance of the $^4A'$ reaction increases and becomes greater than the $^2A'$ reaction above 1.25 eV due to the larger degeneracy factor.

In order to assess the possibility of the $N(^4S)+O_2$ reaction contributing to the dayglow NO emission from CIRRIS 1A[8,9] and the NO emission from the EXCEDE artificial auroral experiment,[24] it is important to establish the NO vibrational-rotational distributions. The calculated NO vibrational distribution at initial translational energies of 0.5 eV and 1.5 eV are shown in Figure 4. At the lowest translational energy (0.5 eV), the vibrational distribution is
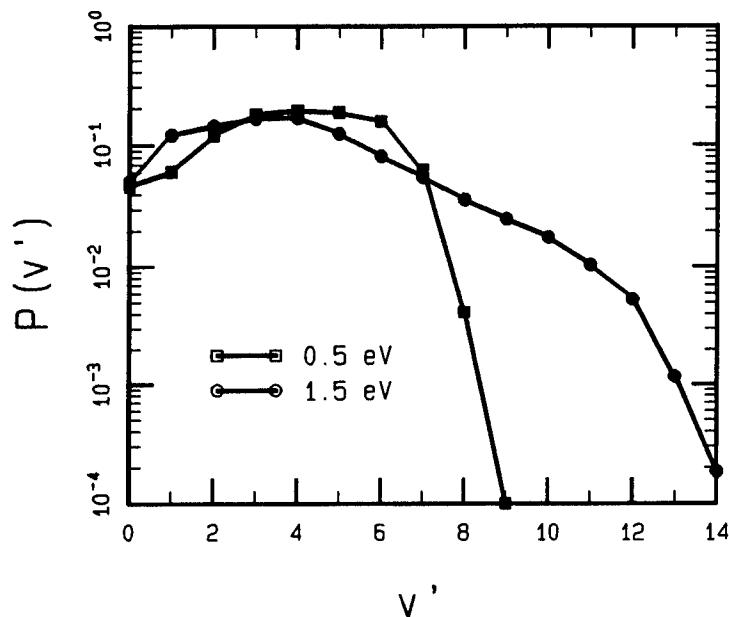
8

Figure 4. NO Vibrational Distribution as a Function of
the Final Vibrational Quantum Number for
Initial Relative Translational Energies of 0.5
and 1.4 eV.

relatively flat from $v'=2$ to $v'=6$ and then rapidly falls off until the maximum vibrational state ($v'=9$) is reached. As E_T is increased to 1.5 eV, the maximum vibrational state populated is $v'=14$. The vibrational distribution peaks around $v'=4$ and then exponentially decreases until $\sim v'=12$. Although the maximum vibrational state populated increases with energy and the shape of the distribution changes, the average vibrational quantum number is nearly constant at a value of 3.9. This behavior results because the average of the distributions from the two potential energy surfaces is almost independent of energy, even though the individual distributions show a modest (and different) energy dependence.

The present results for the $^2A'$ PES are in qualitative agreement with the calculations of Gilibert et al.[11] The largest difference between the calculations is our prediction that the reaction threshold occurs at ~ 0.3 eV, about 0.2 eV lower than the previous calculation. There are also small differences in the NO final vibrational distribution, as the present calculations indicate that the NO is formed with more energy in vibration. This result is due to our $^2A'$ PES

9

being more "attractive" than the surface of Gilibert et al., which has been shown to be an important factor in the vibrational excitation of the reaction products.[25]

There have been three previous measurements of the NO vibrational distribution at room temperature.[14-16] The measurements of Rahbee and Gibson[14] fall off exponentially with increasing NO vibrational quantum number in contrast with the $E_T=0.5$ eV calculation. Herm et al.[15] have pointed out the importance of considering the effects of vibrational quenching. The experiment of Herm et al.[16] shows a NO vibrational distribution which is qualitatively similar to the QCT distribution at $E_T=0.5$ eV, although the experiment indicates a substantial population in the $v'=0$ state. However, again due to vibrational relaxation, it is claimed that the measured distribution only represents a lower bound to the true nascent distribution. An oscillating NO vibrational distribution was obtained in the most recent experiment,[16] which disagrees with previous measurements. Nevertheless, the QCT calculations at 0.5 eV indicate that almost 50% of the available energy goes into vibration, somewhat greater than the experimental observation of 24-34%. Thus, the QCT calculations provide support for the assumption of Herm et al.[15] that previous experiments actually measured a partially relaxed vibrational distribution.
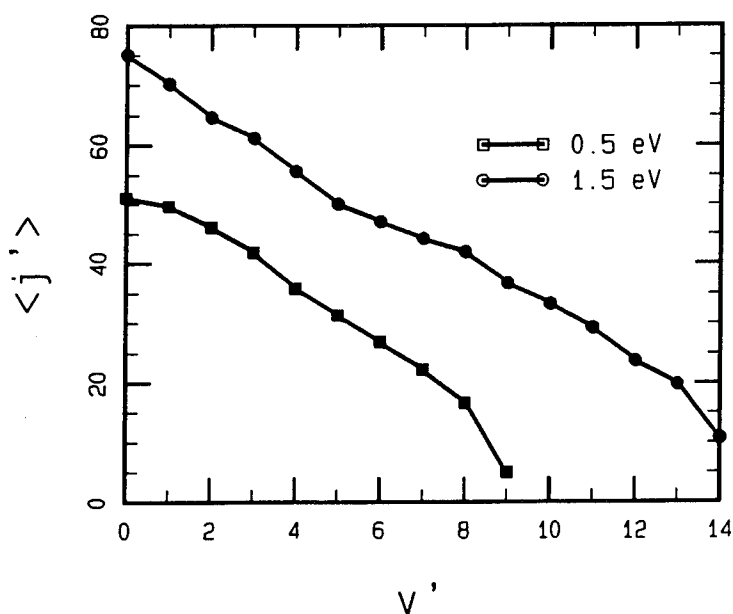

Figure 5.   The Average Rotational Quantum Number, $<J'>$, as a Function of the Final Vibrational Quantum Number v' at Initial Translational Energies of 0.5 and 1.5 eV.

10

Analysis of data from the CIRRIS 1A[9,10] and EXCEDE III[24] observations have shown that NO is formed in the atmosphere with extensive rotational excitation. If the "hot" $N(^4S)+O_2$ reaction is important in NO formation as indicated by Sharma et al.,[8] the QCT calculations should show high rotational excitation. The calculated final average rotational quantum number as a function of final vibrational state is shown in Figure 5 for translational energies of 0.5 eV and 1.5 eV. The large amount of NO rotational excitation indicated by the calculations is completely consistent with the field experiments. The NO rotational distribution, summed over all final vibrational states, can be approximated by a Boltzmann distribution with rotational temperatures of 4000 K and 10000 K at translational energies of 0.5 eV and 1.5 eV, respectively.

Finally, in the analysis of CIRRIS 1A and EXCEDE III NO interferometer data, vibrational populations are determined assuming a single rotational temperature for the complete vibrational manifold.[9,24] Even though Figure 5 shows that this is a poor assumption, the question remains concerning the sensitivity of the NO emission spectrum to the rotational distribution. A NO emission spectrum at a resolution of 2 cm^{-1} using the vibrational-rotational distribution based on the present QCT calculations is shown in Figure 6. The NO vibrational-rotational populations were averaged over a uniform translational energy distribution from 0.3 eV to 2 eV. Ten rotational band heads from the sequence $v' \rightarrow v'-1$ with $v'=1 \rightarrow 10$ are clearly evident, in agreement with the analysis of CIRRIS 1A dayglow spectra by Smith and Ahmadjian.[10] A second NO emission spectrum was calculated using a single effective rotational temperature of 7000 K for each vibrational state. The agreement between this spectrum and the one shown in Figure 6 is excellent, with the largest difference of $\sim 20\%$ for the height of the band heads. Thus, even though each vibrational state possesses very different rotational distribution, the assumption of a single rotational temperature for the complete vibrational manifold in the analysis of NO high resolution emission data is well justified.
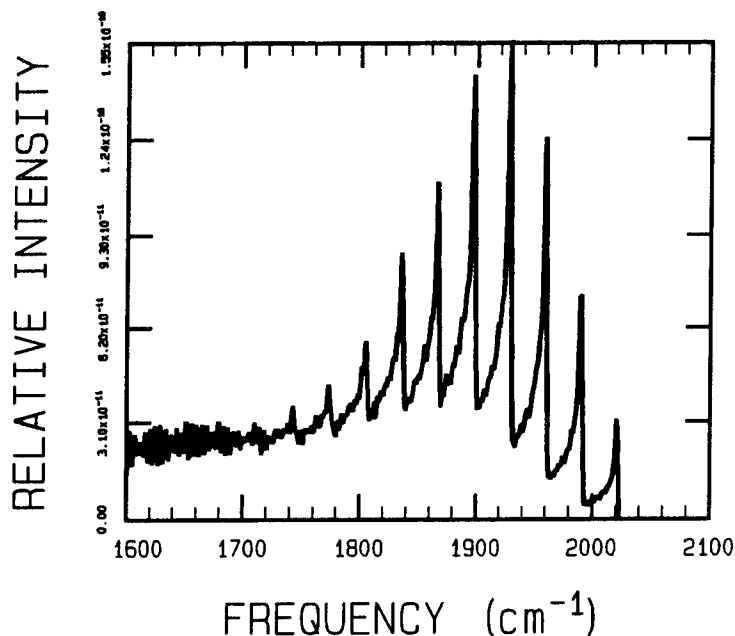
Figure 6. Calculated NO Emission Spectrum at a Resolution of 2 cm^{-1} using the Quasiclassical Reaction Rate for Each Vibrational State with State-Dependent Rotational Temperature.

4. PRELIMINARY ANALYSIS OF NO INTERFEROMETER DATA

The present trajectory studies have provided evidence that the process involving hyperthermal N*(^{4}S) atoms

$$N^*(^4S) + O_2 \rightarrow NO(v,T_r) + O \tag{3}$$

provides significant source of NO which is both highly rotationally and vibrationally excited. In order to access the importance of Reaction (3) in EXCEDE III, we have created a time-dependent kinetics model incorporating a mechanism for producing NO from "hot" N*(^{4}S). The most important inputs for this model is the reaction cross section for the N*(^{4}S)+O$_2$→NO(v,j)+O process, and the quenching of N*(^{4}S) by major atmospheric species.

12

The translational energy of $N^*(^4S)$ is divided into 6 energy bins from 0 to 2 eV $[0 \to 0.0625$ eV, $0.0625 \to 0.125$ eV, $0.125 \to 0.25$ eV, $0.25 \to 0.5$ eV, $0.5 \to 1$ eV, and $1 \to 2$ eV]. The reaction rate constants for $N^*(^4S) + O_2$ from the quasiclassical trajectory calculations are then averaged over translational energy bins from $1 \to 2$ eV, $0.5 \to 1$ eV, and $0.25 \to 0.5$ eV. The various sources, and associated translational energy, of $N^*(^4S)$ from irradiation of the atmosphere are

$$e_p + N_2 \to e_p + N(^4S) + N(^2D,{}^2P) \qquad [0 \to 2 \text{ eV}] \qquad (4)$$

$$N_2^+ + e_s \to aN(^4S) + (2-a)N(^2D) \qquad [1.7 \text{ eV}] \qquad (5)$$

$$O^+ + N_2 \to NO^+ + N(^4S) \qquad [0.75 \text{ eV}] \qquad (6)$$

$$N^+ + O_2 \to O_2^+ + N(^4S) \qquad [1.7 \text{ eV}] \qquad (7)$$

$$NO^+ + e_s \to O + N(^4S) \qquad [1.5 \text{ eV}] \qquad (8)$$

$$O + N(^2D) \to O + N(^4S) \qquad [1.27 \text{ eV}] \qquad (9)$$

$$N^+ + O \to O^+ + N(^4S) \qquad [0.5 \text{ eV}] \qquad (10)$$

$$O + N(^2P) \to O + N(^4S) \qquad [1.9 \text{ eV}] \qquad (11)$$
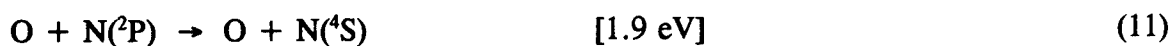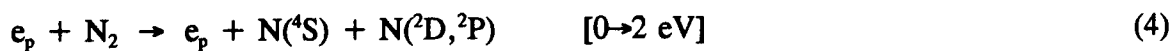
The translational energies from Reactions (4) - (11) are transformed to the $N(^4S) + O_2$ center of mass and placed in the appropriate energy bin. There are estimates of the cross section for the quenching of $N^*(^4S)$, although the uncertainties are unknown. We have chosen a reasonable value of 5×10^{-16} cm^2 for

$$N_i^*(^4S) + M \to N_j^*(^4S) + M \quad . \qquad (12)$$

which is to be compared with the gas kinetic estimate of 3×10^{-15} cm^2. The subsequent cascading of $N^*(^4S)$ translational energy from bin i to i-1 on successive collisions is simply scaled by the relative velocity of each translational energy bin. It has been assumed that each collision of $N^*(^4S)$ with M results in a uniform distribution of the translational energy.[26] The rotationally hot vibrational populations calculated from Reaction (3) are compared to the NO populations

13

obtained from the interferometer data[27] at an altitude of 103 km (upleg) in Figure 7. The excellent agreement between the chemical kinetics model and data provide the first quantitative evidence that Reaction (3) is the source of rotationally hot NO in disturbed atmospheres. Also shown in Figure 7 is a comparison of the vibrational populations obtained from Reaction (1) using the nascent vibrational distribution of Kennealy et al.[28] with the rotationally thermal populations from the interferometer. Again the agreement of the kinetics model and the data is excellent, indicating that the $N(^2D)$ is thermalized at 103 km (upleg).

A similar comparison of the rotationally thermal and hot NO vibrational populations from the model and interferometer data at 115 km (apogee) is shown in Figure 8. For the thermal rotational component, the vibrational populations from the kinetic model are approximately a factor of 3 below the data. This comparison implies that the $N(^2D)$ is probably not thermalized at 115 km, and the rate constant and vibrational distribution used for Reaction (1) is not correct.

In an attempt to account for a hyperthermal $N(^2D)+O_2$ contribution to NO formation, we have created a kinetic model for $N^*(^2D)$ similar to that used for $N^*(^4S)$. The $N(^2D)+O_2$ rate constant was assumed to have a $T^{1/2}$ temperature dependence, which implies an energy
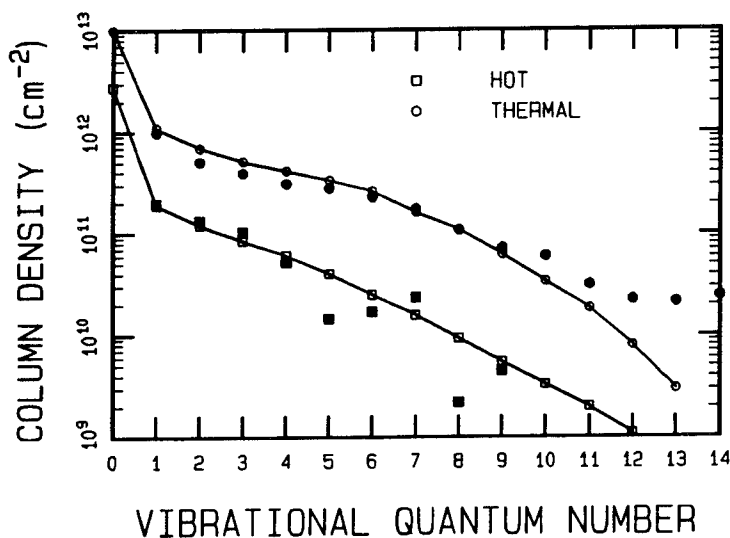

Figure 7. Comparison of the NO Vibrational Populations Derived from the Interferometer Data at an Altitude of 103 km during Upleg with the EXCEDE Kinetic Model Using the Nonthermal $N^*(^2D)+O_2$ and $N^*(^4S)+O_2$ Mechanisms.

independent cross section of 5.7×10^{-17} cm^2 (i.e., appropriate to a reaction with no activation energy). The vibrational populations obtained from the hyperthermal N(^{2}D) kinetic model are compared with the data in Figure 9. It can be seen that the magnitude of the populations from the model is in better agreement with the data, but the vibrational distribution is clearly incorrect. However, recall that the nascent vibrational distribution is based on the room temperature measurements of Kennealy et al.[28], which appears to be inappropriate at collision energies in the 1 to 2 eV range.

Figure 8 also contains a comparison of the rotationally hot vibrational populations from Reaction (3) with the interferometer data. Although the kinetic model is in reasonable agreement with the data, the model underpredicts the vibrational populations for low vibrational quantum numbers. At this altitude (115 km), N(^{4}S) translational energies in the range of 1 to 2 eV is most important for producing NO. As is evident from Figure 3, the ^{4}A' PES makes a significant contribution to the NO vibrational distribution. Unfortunately, the regions of the PES which are most important for determining the vibrational distribution on the ^{4}A' PES are not available from the *ab initio* calculations. Evidently the ^{4}A' PES is more repulsive (i.e., colder NO vibrational distribution) than the PES used in Section 3. Testing of this hypothesis will have to await more extensive *ab initio* calculations.
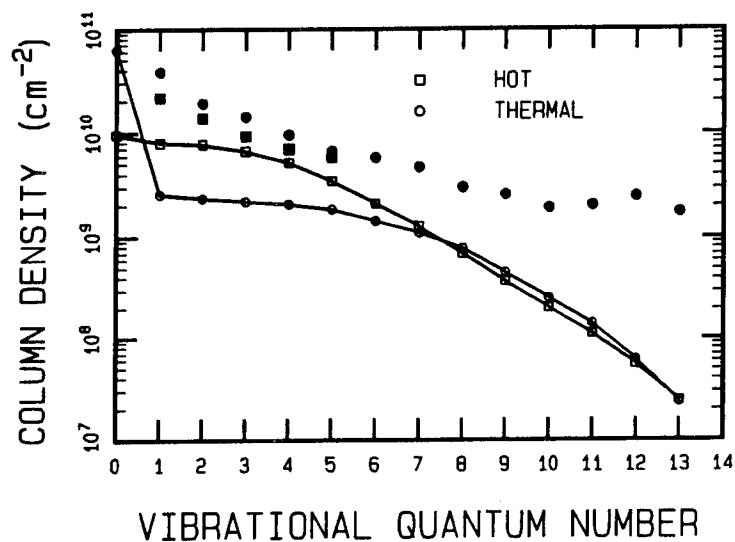
Figure 8.   Comparison of the NO Vibrational Populations Derived from the Interferometer Data at an Altitude of 115 km during Upleg with the EXCEDE Kinetic Model Using the Thermal $N(^2D)+O_2$ and Nonthermal $N^*(^4S)+O_2$ Mechanisms.
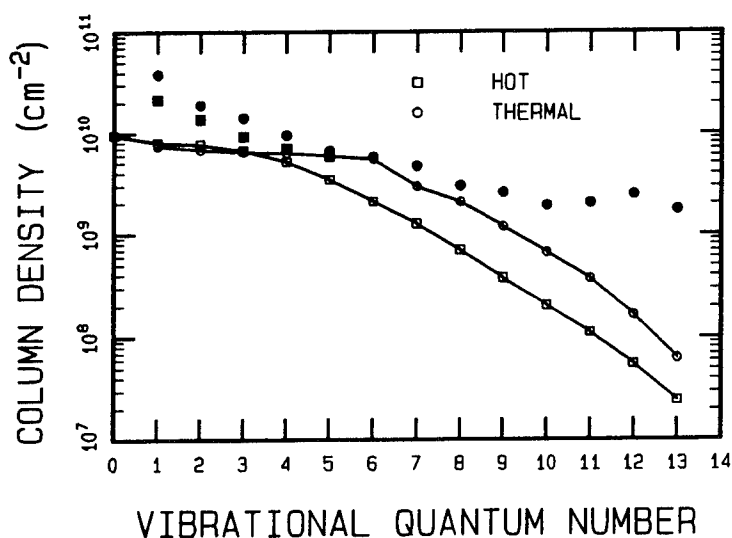

Figure 9.   Comparison of the NO Vibrational Populations Derived from the Interferometer Data at an Altitude of 115 km during Upleg with the EXCEDE Kinetic Model Using the Nonthermal $N^*(^2D)+O_2$ and $N^*(^4S)+O_2$ Mechanisms.

16

5. SUMMARY

This report has provided the first quantitative evidence of the importance of hyperthermal $N(^4S)$ and $N(^2D)$ atoms in the formation of vibrationally and rotationally excited NO. The rate constants and vibrational distributions for rotationally hot NO are obtained from extensive quasiclassical trajectory calculations for the $N(^4S)+O_2(X^3\Sigma_g^-)\rightarrow NO(X^2\Pi)+O(^3P)$ reaction using realistic *ab initio* potential energy surfaces. Good agreement has been obtained with experimental thermal rate constants, indicating that the calculations are a good representation of this reaction. Reaction rate constants and internal NO vibrational-rotational distributions have also been calculated as a function of initial translational energy. The NO vibrational-rotational distributions at low translational energy are consistent with available experimental measurements. Recent field measurement programs observed NO distributions with extensive vibrational excitation characterized by rotational temperatures on the order of 4000 K to 7000 K,[9,24] which the present QCT calculations show are consistent with NO formation from the $N(^4S)+O_2$ reaction.

Quantitative agreement between the chemical kinetics model developed for EXCEDE and the vibrational populations derived from the interferometer data is obtained under conditions of thermalization of nitrogen atoms (i.e., at 103 km under max dose conditions). Analysis of the vibrational populations from the interferometer under other conditions indicate that hyperthermal $N(^2D)$ atoms also play an important role in NO formation. Information concerning the $N(^2D)+O_2$ reaction at hyperthermal translational energies, analogous to that obtained in the present work for the $N(^4S)+O_2$ reaction, is not currently available.

The results of this study indicate that a quantitative understanding of NO formation in the thermosphere will require a detailed investigation into the dynamics of $N(^2D)+O_2$ reaction. Limited *ab initio* studies of the $N(^2D)+O_2$ system have been carried out to characterize the reaction pathways.[29] Although a total of five potential energy surfaces will have to be considered to treat the dynamics of $N(^2D)+O_2$, the calculations are well within the scope of the

quasiclassical trajectory method discussed in this report. Given a more extensive and well chosen set of *ab initio* points for the PES than is currently available, dynamical calculations for this system will be pursued in this laboratory in the future.

6. REFERENCES

1. J.-C. Gérard, "Thermospheric Odd Nitrogen," Planet. Space Sci., 40, 337-353 (1992).

2. L. G. Piper, "The Reactions of N(^{2}P) with O$_2$ and O," J. Chem. Phys., 98, 8560-8564 (1993).

3. M. R. Torr, D. G. Torr, and P. G. Richards, "N(^{2}P) in the Dayglow: Measurement and Theory," Geophys. Res. Lett., 20, 531-534 (1993).

4. E. C. Zipf, P. J. Espy, and C. F. Boyle, "The Excitation and Collisional Deactivation of Metastable N(^{2}P) Atoms in Auroras," J. Geophys. Res., 85, 687-694 (1980).

5. J.-C. Gérard and O. E. Harang, "Metastable N(^{2}P) Atoms in the Aurora," J. Geophys. Res., 85, 1757-1761 (1980).

6. S. Solomon, "The Possible Effects of Translationally Excited Nitrogen Atoms on Lower Thermospheric Odd Nitrogen," Planet. Space Sci., 31, 135-139 (1983).

7. J.-C. Gérard, V. I. Shematovich, and D. V. Bisikalo, "Non Thermal Nitrogen Atoms in the Earth's Thermosphere 2. A Source of Nitric Oxide," Geophys. Res. Lett., 18, 1695-1698 (1991).

8. R. D. Sharma, Y. Sun, and A. Dalgarno, "Highly Rotationally Excited Nitric Oxide in the Terrestrial Thermosphere," Geophys. Res. Lett., 20, 2043-2045 (1993).

9. P. S. Armstrong, S. J. Lipson, J. R. Lowell, W. A. M. Blumberg, D. R. Smith, R. M. Nadile, and J. A. Dodd, "Analysis of Comprehensive CIRRIS 1A Observations of Nitric Oxide in the Thermosphere," Eos Trans AGU, 74, 225 (1993).

10. D. R. Smith and M. Ahmadjian, "Observation of Nitric Oxide Rovibrational Band Head Emissions in the Quiescent Airlow by the CIRRIS-1A Space Shuttle Experiment," Geophys. Res. Lett., 20, 2679-2682 (1993).

11. M. Gilibert, A. Aguilar, M. González, and R. Sayós, "Quasiclassical Trajectory Study of the N(^{4}S$_u$)+O$_2$(X$^3\Sigma_g^-$)$\rightarrow$NO(X$^2\Pi$)+O(^{3}P$_g$) Atmospheric Reaction on the ^{2}A' Ground Potential Energy Surface Employing an Analytical Sorbie-Murrell Potential," Chem. Phys., 172, 99-115 (1993).

12. V. I. Shematovich, D. V. Bisikalo, and J.-C. Gérard, "Non Thermal Nitrogen Atoms in the Earth's Thermosphere 1. Kinetics of Hot N(^{4}S)," Geophys. Res. Lett., 18, 1691-1694 (1991).

13. D. L. Baulch, D. D. Drysdale, and D. G. Haine, Evaluated Kinetic Data for High Temperature Reactions, 2, Butterworths, London (1973).

14. A. Rahbee, J. J. Gibson, "Rate Constants for Formation of NO in Vibrational Levels $v=2$ Through 7 From the Reaction $N(^4S)+O_2 \rightarrow NO^\ddagger + O$," J. Chem. Phys., 74, 5143-5148 (1981).

15. R. R. Herm, B. J. Sullivan, and M. E. Whitson, Jr., "Nitric Oxide Vibrational Excitation From the $N(^4S)+O_2$ Reaction," J. Chem. Phys., 79, 2221-2230 (1983).

16. I. C. Winkler, R. A. Stachnik, J. I. Steinfeld, and S. M. Miller, "Determination of $NO(v=0-7)$ Product Distribution From the $N(^4S)+O_2$ Reaction Using Two-Photon Ionization," J. Chem. Phys., 85, 890-899 (1988).

17. J.-C. Gérard, V. I. Shematovich, D. V. Bisikalo, "Effect of Hot $N(^4S)$ Atoms on the NO Solar Cycle Variation in the Lower Thermosphere," J. Geophys. Res., 98, 11581-11586 (1993).

18. Ø. Lie-Svendsen, M. H. Rees, K. Stamnes, and E. C. Whipple, Jr., "The Kinetics of "Hot" Nitrogen Atoms in Upper Atmosphere Neutral Chemistry," Planet. Space Sci., 39, 929-943 (1991).

19. S. P. Walch and R. L. Jaffe, "Calculated Potential Surfaces for the Reactions: $O+N_2 \rightarrow NO+N$ and $N+O_2 \rightarrow NO+O$," J. Chem. Phys., 86, 6946-6956 (1987).

20. R. L. Jaffe, M. Pattengill, and D. W. Schwenke, "Classical Trajectory Studies of Gas Phase Reaction Dynamics and Kinetics Using ab initio Potential Energy Surfaces," in Supercomputer Algorithms for Reactivity, Dynamics, and Kinetics of Small Molecules, edited by A. Laganá, pp. 367-382, Kluwer, Dordrecht (1989).

21. D. G. Truhlar and J. T. Muckerman, "Reactive Scattering Cross Sections III: Quasiclassical and Semiclassical Methods," in Atom-Molecule Collision Theory, edited by R. B. Bernstein, pp. 505-566, Plenum, New York (1979).

22. K. S. Sorbie and J. N. Murrell, "Analytical Potentials for Triatomic Molecules from Spectroscopic Data," Mol. Phys., 29, 1387-1407 (1975).

23. P. Brumer, "Stability Concepts in the Numerical Solution of Classical Atomic and Molecular Scattering Problems," J. Comp. Phys., 14, 391-419 (1974).

24. S. J. Lipson, P. S. Armstrong, J. R. Lowell, W. A. M. Blumberg, D. E. Paulsen, M. J. Fraser, W. T. Rawlins, D. B. Green, R. E. Murphy, and J. A. Dodd, "Mission-Wide EXCEDE III Nitric Oxide Spectroscopic Analysis," Eos Trans AGU, 74, 225 (1993).

25. P. J. Kuntz, E. M. Nemeth, J. C. Polanyi, S. D. Rosner, and C. E. "Energy Distribution Among Products of Exothermic Reactions. II. Repulsive, Mixed, and Attractive Energy Release," J. Chem. Phys., 44, 1168-1184 (1966).

26. J. A. Logan and M. B. McElroy, "Distribution Functions for Energetic Oxygen Atoms in the Earth's Lower Atmosphere," Planet. Space Sci., 25, 117-122 (1977).

27. W. T. Rawlins and B. D. Green, Private Communication, Physical Sciences, Inc., February, 1994.

28. J. P. Kennealy, F. P. Del Greco, G. E. Caledonia, and B. D. Green, "Nitric Oxide Chemiexcitation Occurring in the Reaction between Metastable Nitrogen Atoms and Oxygen Molecules," J. Chem. Phys., 69, 1574-1584 (1978).

29. H. H. Michels, "Radiative/Kinetic Properties of Debris Oxides and Air Molecules," Presented at the DNA/RACE AESOP Meeting (August, 1990).